Ecological Modelling 329 (2016) 5–17

Contents lists available at ScienceDirect

Ecological Modelling

journal homepage: www.elsevier.com/locate/ecolmodel

A cellular automaton model for grasshopper population dynamics in Inner Mongolia steppe habitats

Na Zhang[a,b,*], Yong-Cai Jing[a], Cheng-Yu Liu[a], Yao Li[a], Jing Shen[a]

[a] College of Resources and Environment, University of Chinese Academy of Sciences, Beijing 101408, China
[b] Huairou Eco-Environmental Observatory, Chinese Academy of Sciences, Beijing 101408, China

ARTICLE INFO

Article history:
Received 13 August 2015
Received in revised form 11 February 2016
Accepted 1 March 2016
Available online 17 March 2016

Keywords:
Oedaleus decorus asiaticus
Grasshopper density
Dispersal
Aboveground biomass
Grasshopper–plant interaction
Spatial heterogeneity

ABSTRACT

We developed a cellular automaton model for the spatiotemporal dynamics of grasshopper (*Oedaleus decorus asiaticus*) populations with a density of 3–12 ind m^{-2} in a typical semiarid steppe. The model simulates grasshopper dynamics within each cell and dispersal between adjacent cells at each time step from the completion of hatching to ovipositing. After the model parameters were obtained or calibrated, the natural growth of grasses (the preferred food of *O. d. asiaticus*), and their variation after being fed on by cattle and grasshoppers, were modeled to explore grasshopper–plant interactions. Dispersal rules were formulated by considering the abundance of grasshoppers and grasses and their interactions within both potential source and sink cells, habitat conditions of sink cells, and spatial isolation (or connectedness) between source and sink cells. A case study was conducted at a sample landscape in Xianghuangqi County, Inner Mongolia, China. The temporal variations of the modeled grass biomass and grasshopper density were consistent with actual variations. The modeled densities were within the measured ranges for most of the cells. The estimation accuracy was higher for the 4th and 5th instars than for adults, and was higher for cells with higher initial densities (not lower than 3 ind m^{-2}). The modeled results showed that the main factors influencing grasshopper density differed for different instars. During the 2nd and 3rd instar, grasshopper density depended on the number of hatched nymphs and their mortality. During the 4th instar, habitat suitability determined the density threshold that caused grasshoppers to disperse and the potential sink or source cells. This resulted in different density variations between the cells with initial densities >6.0 ind m^{-2} and those with densities <6.0 ind m^{-2}. During and after the 5th instar, grasshopper density was very stable due to the slightly decreasing habitat suitability. The modeled results are expected to provide a scientific basis for predicting grasshopper dynamics and controlling grasshopper plagues in heterogeneous spaces.

1. Introduction

The Inner Mongolian grasslands are the largest in China and represent a typical Eurasian semiarid ecosystem. Over the past few decades, desertification due to climate change and overgrazing has deteriorated these grasslands, creating favorable habitats for grasshoppers. Since 2000, grasshopper outbreaks have been common across large areas (Liu and Guo, 2004; Zhang et al., 2015). Therefore, it is necessary to precisely predict the location, scope, and degree of grasshopper infestations (Shen et al., 2015; Zhang et al., 2015).

A number of studies have been conducted on grasshopper physiology and ecology in Inner Mongolia (e.g., Chen et al., 2006; Fan et al., 1997; Kang and Chen, 1992; Lu et al., 2005; Ma, 1964). However, most studies have focused on temporal and not on the spatial dynamics. Studies on dynamics have been conducted within individual plots or patches, whereas dynamic models presuppose homogeneity and should be considered point models without any spatial extension. Furthermore, most of these studies did not explicitly link ecological processes to spatial patterns, limiting their ability to provide insights into spatial grasshopper–plant interactions. Nonetheless, such spatial patterns are crucial for understanding and predicting population changes (Chen et al., 2011).

Modeling the spatial dynamics of a population is an ambitious and often a challenging task. Early models introduced the concept of reaction-diffusion systems from physical sciences and used partial differential equations to describe the spatiotemporal dynamics

* Corresponding author at: College of Resources and Environment, University of Chinese Academy of Sciences, No. 380, Huaibei Town, Huairou District, Beijing 101408, China. Tel.: +86 10 69672842.
E-mail address: zhangna@ucas.ac.cn (N. Zhang).

http://dx.doi.org/10.1016/j.ecolmodel.2016.03.002
0304-3800/

of state variables (Blackwell, 2007). However, because they assume processes are homogeneous, these early models failed to consider the effects of spatial heterogeneity and local spatial interactions that could be crucial to understanding complex ecosystem dynamics (Chen et al., 2011).

Cellular automata (CA) are a class of complex system models that allow spatially explicit ecological processes to be simulated (Cannas et al., 1999; Hogeweg, 1988; Perry and Enright, 2007; Vinatier et al., 2011; Wang et al., 2003). CA models typically consist of a grid of discrete cells with explicit spatial locations. Each cell is characterized by finite and discrete states describing physical or biological properties. The states of a cell are updated at discrete time steps according to a set of local transition rules that depend on the states of the cell and its neighbors (Balzter et al., 1998). Spatial heterogeneity is exhibited by specifying the related spatial representations of each cell and the spatial relationships between adjacent cells. In addition, a CA model simulates spatiotemporal evolution in a "bottom-up" approach (Grimm et al., 2005; Li et al., 2007). This approach focuses on dynamic processes at a local scale, from which the dispersion pattern at a landscape scale may emerge collectively over time.

Dispersal is important for flying insect populations to survive unsuitable habitat conditions or overcrowding (Ciss et al., 2013) but is often difficult to measure. With simple computational rules and an explicitly spatial approach, CA approaches have been applied to modeling insect populations, with dispersal or the outbreak process as a primary focus. Zhou and Liebhold (1995) developed a series of CA transition probability models to predict the spatial dynamics of gypsy moth (*Lymantria dispar* L.) outbreaks. By incorporating neighboring locations, spatial variation in forest susceptibility or defoliation frequencies, and egg mass counts in their models, they could increase the precision and accuracy of predictions. Pukkala et al. (2014) developed a CA model for the potential spread of the pinewood nematode (*Bursaphelenchus xylophilus*) in Europe by human-mediated transportation, flight direction and distance from its carriers in pine forests, and climate change. Bone et al. (2006) revealed that tree mortality patterns caused by infestations of mountain pine beetle (MPB) could be modeled using a fuzzy-constrained geographical information systems (GIS)-based CA model. Simpson et al. (1999) stated that CA models allow the mechanisms by which vegetation distribution at a local scale affects population dynamics to be explored.

In our study, we constructed a CA model of the single species population dynamics of *Oedaleus decorus asiaticus* Bei-Bienko in a steppe habitat. The main aim was to investigate what in the environment drives the evolution of grasshopper abundance (temporal pattern) and distribution (spatial pattern), and from which the transition rules (especially dispersal rules) were formulated. Although the present study focuses on model design, not model implementation, we used a case study as model validation.

2. Material and methods

2.1. Study area and grasshopper species

The study area was in Xianghuangqi County, Inner Mongolia (41°56′–42°45′ N, 113°32′–114°45′ E). The climate, terrain, vegetation, and soil conditions have been described in Shen et al. (2015) and Zhang et al. (2015).

The area was mostly dominated by the grasshopper species *O. d. asiaticus*, but *Dasyhippus barbipes* Fischer-Waldheim, *Bryodema luctuosum* Stoll, and *Myrmeleotettix palpalis* Zubowsky were also present. The present study considered only *O. d. asiaticus*, a primary pest in the grasslands of the northern China. *O. d. asiaticus* is an oligophagous insect that prefers feeding on grass, including *Stipa krylovii* Roshev., *S. grandis* P.A. Smirn., *Cleistogenes squarrosa* (Trin.) Keng, and *Leymus chinensis* (Trin.) Tzvelev (Chen, 2007).

O. d. asiaticus is univoltine. Generally, the 4th and 5th instar nymphs and adults occur in early July and the density peaks in mid- to late July. Adults oviposit in the top 5 cm of the soil in late July or early August, dying soon thereafter. Eggs have an obligatory diapause that lasts the entire winter, and nymphs hatch in early to mid-June the following year (Chen, 2007; Zhou et al., 2012).

The morphological characteristics of *O. d. asiaticus* determine its dispersal ability (Yan and Chen, 1998). The 1st, 2nd, and 3rd instar nymphs often move between adjacent land surfaces within a site, whereas the 4th and 5th instar nymphs and adults may fly to other sites and landscapes within a 15-km range (Chen, 2007). Adults seldom migrate beyond 15 km.

2.2. Cellular automaton model description

2.2.1. Cellular space

The cellular space is a relatively closed system, which means that *O. d. asiaticus* individuals move mostly within the space defined and outside individuals rarely enter the space. It is defined as a regular or irregular two-dimensional matrix of identical square cells. A cell is a modeling unit with spatially homogeneous physical and biological conditions in which individuals can mingle. A GIS raster-based environment provides a spatial framework for discrete cells in the CA model.

O. d. asiaticus individuals disperse uniformly randomly within a cell at any time, but form clusters (social groups) over the cellular space, mostly resulting from spatial heterogeneity in environmental characteristics, especially patches where plants are clumped together. Given that our aim is to explore the spatial dynamics of grasshopper populations within the space, the cell (a homogeneous spatial unit) size should be smaller than the smallest scale of relevant environmental heterogeneity (the size of habitat patches) or the range over which local spatial association of individuals occur (the characteristic scale of local dispersal). Meanwhile, the space extent should be larger than this characteristic scale (Berec, 2002; Dungan et al., 2002).

We conducted a field experiment on the spatial aggregation of *O. d. asiaticus* individuals at a typical sample plot in Aobaoyingol village. Moran's *I* correlogram of *O. d. asiaticus* density showed that individuals were strongly clumped within a range of about 180 m × 180 m surrounding a site, which was the characteristic scale of local dispersal (data not shown). When the range changed from 180 to 210 m, the individuals were randomly distributed. When the range reached 210 m, individuals became widely dispersed. Hence, the cell size should not be larger than 180 m × 180 m and the space extent should not be smaller than 180 m × 180 m.

Cells located near the space boundary have incomplete interactions with neighbors than those in the middle of the space. This phenomenon, termed the edge effect, is a common model artifact (Berec, 2002). To reduce the edge effect, the space is artificially expanded to more cells surrounding the actual edge cells. Therefore, the edge cells become the central ones within their discrete neighbors, so that they have complete interaction with neighbors and can be simulated. Given that the expanded cells outside the boundary are not the actual ones, environmental conditions and grasshopper abundance and behaviors within these cells are considered the same as those within the nearest actual edge cells. The population dynamics within these expanded cells are also simulated, but the results are not analyzed and exhibited.

2.2.2. Neighborhood

The neighborhood refers to the cells in a defined area surrounding each cell that may influence the state of that cell during the next time step. The model assumes that the individuals within a

cell interact with others within the same neighborhood. The model formulates regular square-shaped neighborhoods in terms of rings of the eight nearest cells, following a Queen's move definition. The neighborhood size cannot exceed the actual range of influence of the focal cell, which is the local spatial association and/or dispersal distance of *O. d. asiaticus* individuals (180 m); if it does, the cell size should be decreased. The four orthogonal neighbors and four completely diagonal neighbors of a cell differ due to the difference in their distances to the cell, which may affect grasshopper dispersal.

2.2.3. Time

The CA model spans the time from the completion of hatching (after early or mid-June) to the completion of ovipositing (after early or mid-August) of *O. d. asiaticus*. Temporal grain is represented as a time step with a regular interval that is finer than the resolution at which the time-step-dependent processes take place. Given that the same instars last for a minimum of about six days, temporal grain may range from one day to five days.

2.2.4. Cell states

Grasshopper occurrence is particularly associated with the type, abundance, and distribution of grasses (Ni, 2002; Torrusio et al., 2002). In the CA model, cell B_{ij}, which is located with i and j coordinates at time step t, takes on the two discrete states: the density of *O. d. asiaticus* (N_{ij}^t) and the aboveground biomass of grass species (G_{ij}^t) :

$$S_{ij}^t = (N_{ij}^t, G_{ij}^t) \tag{1}$$

N_{ij} and G_{ij}, and thus the states of a cell, vary with the growing season.

2.2.4.1. Grass aboveground biomass. The values of G_{ij} at the time t_0 are typically generated from measured data or inversed remote sensing data or measured vegetation coverage. If there is no human and natural disturbance, G_{ij} is well approximated by the logistic model of population growth during the growing season:

$$\frac{dG_{ij}}{dt} = rG_{ij}\left(1 - \frac{G_{ij}}{K}\right) \tag{2}$$

$$G_{ij}(t) = \frac{K}{1 + \exp(a - rt)} \tag{3}$$

$$a = \ln \frac{K - G_{ij}^{t_0}}{G_{ij}^{t_0}} \tag{4}$$

where t is the time step in day; r is the intrinsic growth rate of the grasses; K is the carrying capacity of the grasses; and $G_{ij}^{t_0}$ is the initial G_{ij}. The values of the parameters r and K are usually estimated as averages from observed or derived information and are thus identical over the entire space.

In the CA model, G is estimated for each of the three periods, first without considering the influence of disturbance. From t_0 to t_1, a logistic equation is used to model the rising trends in G. From t_1 to t_2, according to general field observations, G peaks and remains high, with little variation, for more than a few days. From t_2 to t_3, G rapidly decreases as the grasses wither, and it is assumed that G decreases linearly with seasonal variation.

G is also affected by grasshopper food consumption and livestock grazing. The amount that grasshoppers consume is closely associated with individuals' instar and population density. *O. d. asiaticus* is assumed to have the same forage preference for the four main grasses (*S. krylovii*, *S. grandis*, *C. squarrosa*, and *L. chinensis*), and thus these grasses are not differed. The probability that the grasses are consumed is assumed to completely depend on their aboveground biomass.

Livestock such as sheep and cows in the study area mainly feed on *S. krylovii*, *S. grandis*, *C. squarrosa*, *L. chinensis*, *Agropyron cristatum* (L.) Gaertn., *Allium polyrhizum* Turcz., and *A. mongolicum* Regel. Livestock need to consume a large quantity of grasses to meet their nutritional requirements in this semiarid grassland, where the most dominant plants are grasses and there are only a small number of other plants. However, livestock partially consume or avoid consuming certain grasses such as *S. krylovii* because of its inferior palatability. In the model, both the potential consumption and forage preference estimate the probability that livestock consume grasses. It is assumed that the probability that grasses are encountered is approximately equal to the proportion of the aboveground biomass of the main grasses relative to all the grasses and forbs that are available to livestock (f); the probability that grasses are eaten after they are encountered (p') is 0.9, on the basis of their palatability. Thus, the final probability that livestock consume grasses is $p'f$.

Accordingly, the variation in G at time step t ($G_{ij}(t)$) with grasshopper density and grazing intensity may be expressed as:

$$G_{ij}(t) = \begin{cases} G_{ij}^{t_0} & t = t_0 \\ \dfrac{K}{1 + e^{a - rt}} - \displaystyle\sum_{t=t_0}^{t-1} N_{ij}(t) \cdot k(t) - p' \cdot f_{ij}^1 \cdot \beta_{ij}^1 \cdot t & t_0 < t \le t_1 \\ G_{ij}^{t_1} - \displaystyle\sum_{t=t_1}^{t-1} N_{ij}(t) \cdot k(t) - p' \cdot f_{ij}^1 \cdot \beta_{ij}^1 \cdot (t - t_1) & t_1 < t \le t_2 \\ G_{ij}^{t_2} - \displaystyle\sum_{t=t_2}^{t-1} N_{ij}(t) \cdot k(t) - p' \cdot f_{ij}^2 \cdot \beta_{ij}^2 \cdot (t - t_2) - \gamma_{ij} \cdot (t - t_2) & t_2 < t \le t_3 \end{cases} \tag{5}$$

where $k(t)$ is the daily amount eaten by *O. d. asiaticus* at time step t (g ind^{-1} d^{-1}); β_{ij} is the daily amount eaten by livestock within cell B_{ij} (g ind^{-1} d^{-1}); and γ_{ij} is the natural withering rate of main grasses within cell B_{ij} at the end of the growing season (g m^{-2} d^{-1}). f_{ij}^1 and β_{ij}^1 are the values during the period that G is increasing, and f_{ij}^2 and β_{ij}^2 are the values during the period that G is declining.

The values for $k(t)$, f_{ij}^1, and f_{ij}^2 are available or can be estimated from observed information. The unknown parameters β_{ij}^1, β_{ij}^2, and γ_{ij} have relatively independent effects on G_{ij}, so they may be calibrated independently. By adjusting their values, it is possible to fit the curve that is formulated by Eq. (5) to the observed values during the growing period of main grasses.

2.2.4.2. Density of Oedaleus decorus asiaticus. The values of N_{ij} at the initial time t_0 ($t = 0$) (after the completion of hatching) are typically generated from observed patterns of individuals or evaluated potential habitat suitability. The model assumes that no new nymphs hatch after t_0, so the reproduction process does not exist over all the time steps for this univoltine species. The processes that drive spatiotemporal dynamics mainly include growth and mortality, grasshopper–plant interactions, and dispersal. Generally, weather conditions over the time steps exhibit relatively stable variations with the season, so the effects of extreme weather on these processes have not been considered.

O. d. asiaticus individuals are homogeneously mixed and distributed within a cell so that any individual may equally interact with any other. All the individuals over the cellular space are considered to be in the same instar and have identical behaviors and appearances at the same time step. They are not subject to mortality during a given instar, and simultaneously develop to the next instar with a density-independent probability of uniform mortality. The 1st, 2nd, and 3rd instar nymphs stay within their birth cells, and records are kept only for the surviving nymphs. The late-instar nymphs and adults may disperse between cells, so the dispersal rules are applied to the surviving individuals.

2.2.5. Dispersal rules

Generally, dispersal between sites is needed for effective survival for the late-instar nymphs or adults of *O. d. asiaticus* in temporary habitats. The cells in which resources are available change with the space and time, and *O. d. asiaticus* individuals, as active feeders, can move from one cell to another. The main factors that contribute to whether they move, how many of them move, and where they can move include *O. d. asiaticus* abundance, the grass biomass on which they feed, and the interactions of these two factors within both potential source and sink cells, as well as habitat conditions of sink cells and spatial isolation (or connectedness) between source and sink cells (Fig. 1).

2.2.5.1. Grasshopper habitat suitability. The main habitat factors that affect grasshopper occurrence and movement include terrain, soil, and vegetation. These factors are spatially heterogeneous over the cellular space. They are generally fixed, although soil volumetric water content (SVWC), vegetation type, and vegetation coverage may vary seasonally. These factors may be obtained by field experiments, spatial interpolation from a finite number of measured samples, or the use of remote sensing data or other digitalized maps in a GIS environment.

A fuzzy theory approach explains the inherent spatial uncertainties and overcomes problems with incomplete knowledge to reveal the influence of habitat on grasshopper occurrence and dispersal. Fuzzy sets and fuzzy logic have been applied to challenges such as analyzing land suitability (Davidson et al., 1994), determining tree susceptibility to attack by mountain pine beetles (Bone et al., 2006), and evaluating the habitat suitability for grasshoppers (Ni, 2002; Zhang et al., 2015). Shen et al. (2015) constructed a GeogDetector-based fuzzy model system based on that of Zhang et al. (2015), where the habitat suitability level for *O. d. asiaticus* was a function of the effects of individual habitat factors (P_1) and interactions between any two factors on grasshopper density (P_2) and the fuzzy membership (Q). Q was defined as the probability that a habitat category is associated with a given grasshopper density rank: 'very high,' 'high,' 'low,' or 'very low.' The data processing software Excel-GeogDetector (Wang et al., 2010; Wang and Hu, 2012) was used to obtain P_1 and P_2. Both of the models reliably indicated the potential occurrence of *O. d. asiaticus* over the entire county studied. In the CA model, the habitat suitability (high, medium, or low) obtained for each cell at each time step provides the input for the dispersal rules.

In addition, the habitat suitability levels obtained before nymphs move to other cells during the early growing season can be used to estimate the initial grasshopper densities (ranks) when measured densities are unavailable.

2.2.5.2. Source cells and sink cells. Grasshopper dispersal is often directed, so it is necessary to identify source and sink cells. If grasshopper density is very high or if the aboveground biomass of the main grasses on which they feed is very low within a cell, the 1st, 2nd, and 3rd instar nymphs may die, and the late-instar nymphs and adults may move to neighboring cells. The threshold densities (N_{ts}) causing *O. d. asiaticus* individuals to disperse are determined for all the cells on the basis of their habitat suitability levels. Cells with higher habitat suitability levels are expected to have more individuals and thus higher N_{ts}. The threshold aboveground biomass of grasses (G_{ts}) causing individuals to disperse is also determined. If $N_{ij}(t) \geq N_{ts}$ or $G_{ij}(t) < G_{ts}$ within cell B_{ij}, then B_{ij} can be a source cell, i.e., *O. d. asiaticus* may move from B_{ij} to the neighboring cells. If $N_{ij}(t) < N_{ts}$ and $G_{ij}(t) \geq G_{ts}$ within cell B_{ij}, then B_{ij} can be a sink cell; that is, individuals from neighboring cells may enter B_{ij}.

2.2.5.3. Emigration from source cells. It is assumed that *O. d. asiaticus* individuals emigrate from source cell B_{ij} only when a sink cell is adjacent to B_{ij}. If the individuals cannot emigrate, they remain in their original cell. The proportion of the total number of individuals in a source cell B_{ij} ($\delta_{ij}(t)$) that emigrate is used to estimate the total emigration ($R_{ij}(t)$):

$$R_{ij}(t) = \delta_{ij}(t) \cdot N_{ij}(t) \cdot A \tag{6}$$

where A is the area of a cell (m^2).

The value of $\delta_{ij}(t)$ is probabilistic. The Mersenne Twister algorithm developed by Matsumoto and Nishimura (1998) was used to generate pseudorandom numbers of $\delta_{ij}(t)$. It was designed specifically to rectify most of the flaws in the older generators. It rapidly generates high-quality pseudorandom integers.

To obtain $\delta_{ij}(t)$, it is necessary to follow these two principles regarding resource availability:

(1) After individuals emigrate, the *O. d. asiaticus* density within cell B_{ij} should not exceed the threshold value (N_{ts}) for B_{ij}:

$$0 \leq N_{ij}(t) - \delta_{ij}(t) \cdot N_{ij}(t) < N_{ts} \tag{7}$$

which yields the following equation:

$$\frac{N_{ij}(t) - N_{ts}}{N_{ij}(t)} < \delta_{ij}(t) \leq 1 \tag{8}$$

(2) Aboveground biomass of *S. krylovii* within cell B_{ij} should not be lower than the amount consumed by the remaining *O. d. asiaticus* individuals:

$$(N_{ij}(t) - \delta_{ij}(t) \cdot N_{ij}(t))k(t) \leq G_{ij}(t) \tag{9}$$

which yields the following equation:

$$\delta_{ij}(t) \geq 1 - \frac{G_{ij}(t)}{N_{ij}(t) \cdot k(t)} \tag{10}$$

2.2.5.4. Effect of spatial isolation between cells on grasshopper dispersal. The probability that *O. d. asiaticus* individuals emigrate from a source cell to its orthogonal and completely diagonal neighbors, and the distances that they travel may differ considerably depending on spatial isolation. The distance between a cell and its orthogonally adjacent cells is set at 1, and thus the distance between a cell and its diagonally adjacent cells is $\sqrt{2}$. The number of migrating individuals is supposed to exhibit an inversely exponential relationship with distance.

$$\begin{cases} p \cdot m + q \cdot n = R_{ij}(t) \\ p = \exp(\sqrt{2} - 1) \cdot q \end{cases} \tag{11}$$

where m and n are the numbers of the sink cells orthogonally and completely diagonally adjacent to a source cell, respectively; p and q are the numbers of individuals that may migrate from a cell to an orthogonally and completely diagonally adjacent cell, respectively. The values of p and q can be obtained from Eq. (11):

$$\begin{cases} p = \dfrac{\exp(\sqrt{2} - 1) \cdot R_{ij}(t)}{(n + \exp(\sqrt{2} - 1) \cdot m)} \\ q = \dfrac{R_{ij}(t)}{(n + \exp(\sqrt{2} - 1) \cdot m)} \end{cases} \tag{12}$$

The total numbers of individuals that may migrate from a cell to its orthogonally and diagonally adjacent cells are pm and qn, respectively.

2.2.5.5. Effect of habitat suitability of cells on grasshopper dispersal. Cells with higher habitat suitability should be more attractive to grasshoppers and are more likely to become sink cells, disregarding the differences in other factors that may influence grasshopper

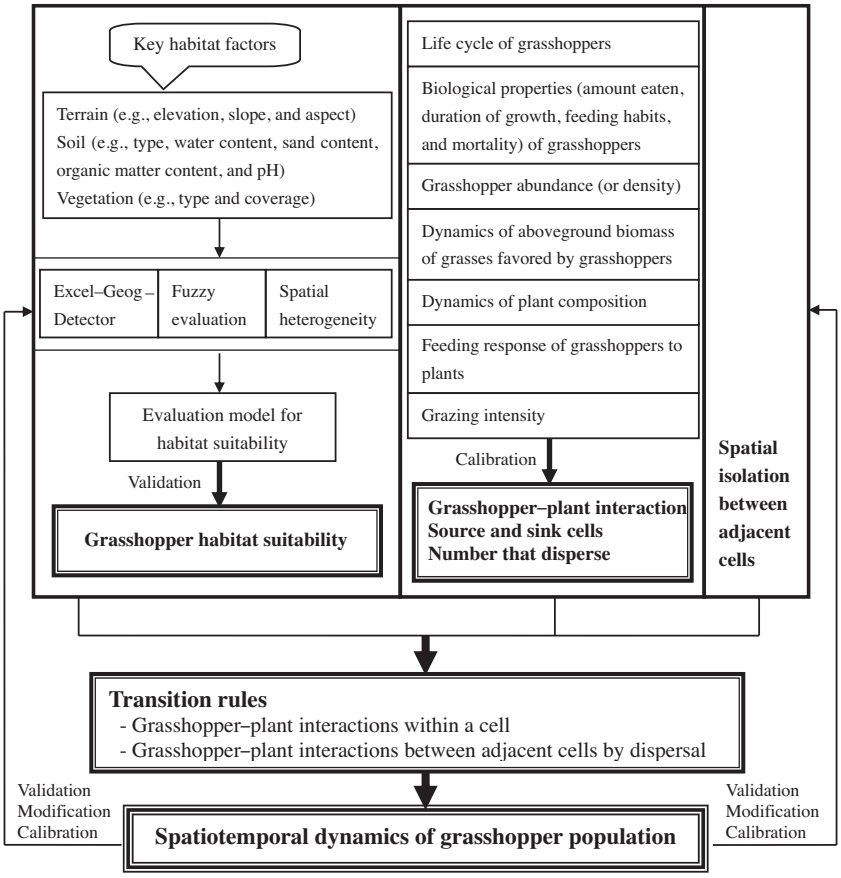

Fig. 1. Conceptual diagram of the constructed cellular automaton model of the dynamics of grasshopper populations.

dispersal. More individuals generally occur within cells with higher habitat suitability during any given period. Therefore, the probability that an individual will move to an adjacent cell depends on the grasshopper density corresponding to the habitat suitability of the adjacent cell.

$$\begin{cases} P_3 = \mathrm{AGD}_3/(\mathrm{AGD}_3 \times S_3 + \mathrm{AGD}_2 \times S_2 + \mathrm{AGD}_1 \times S_1) \\ P_2 = \mathrm{AGD}_2/(\mathrm{AGD}_3 \times S_3 + \mathrm{AGD}_2 \times S_2 + \mathrm{AGD}_1 \times S_1) \\ P_1 = \mathrm{AGD}_1/(\mathrm{AGD}_3 \times S_3 + \mathrm{AGD}_2 \times S_2 + \mathrm{AGD}_1 \times S_1) \\ P_3 = \mathrm{AGD}_3/(\mathrm{AGD}_3 \times s_3 + \mathrm{AGD}_2 \times s_2 + \mathrm{AGD}_1 \times s_1) \\ P_2 = \mathrm{AGD}_2/(\mathrm{AGD}_3 \times s_3 + \mathrm{AGD}_2 \times s_2 + \mathrm{AGD}_1 \times s_1) \\ P_1 = \mathrm{AGD}_1/(\mathrm{AGD}_3 \times s_3 + \mathrm{AGD}_2 \times s_2 + \mathrm{AGD}_1 \times s_1) \end{cases} \quad (13)$$

where S_3, S_2, and S_1 are the number of orthogonally adjacent cells with high, medium, and low habitat suitability, respectively, for source cell B_{ij}; P_3, P_2, and P_1 are the probabilities that grasshoppers may move from B_{ij} to one of these orthogonally corresponding cells; s_3, s_2, and s_1 are the number of completely diagonally adjacent sink cells with high, medium, and low habitat suitability, respectively, for source cell B_{ij}; p_3, p_2, and p_1 are the probabilities that grasshoppers may move from B_{ij} to one of these completely diagonally corresponding cells; and AGD_3, AGD_2, and AGD_1 are the average grasshopper densities over the cellular space, corresponding to high, medium, and low habitat suitability, respectively.

The number of individuals that finally move to orthogonally adjacent cells with a certain habitat suitability may be estimated from the product of pm and P_3S_3, P_2S_2, or P_1S_1. The number of individuals that finally move to diagonally adjacent cells with a certain habitat suitability may be estimated from the product of qn and p_3s_3, p_2s_2, or p_1s_1.

2.2.6. Computer program realization

The CA model was compiled using IDL (interactive data language) to estimate *O. d. asiaticus* density within each cell at each time step. The time series of density maps forms a movie showing the dynamics of *O. d. asiaticus* over the entire space. IDL is a trusted scientific programming language, and has been applied widely in space science to process large amounts of data and extract meaningful visualizations from complex numerical data. The syntax includes many constructs from Fortran and some from C language.

3. A case study

3.1. Sample landscape and field surveys

A grazing steppe of around 12.6 km^2 located in Aobaoyingol village (42°12′11–42°14′42″ N, 114°07′34″–114°11′02″ E) was selected (Fig. 2). Its southern area was near Huanghua mountain, northern area was blocked by a 10-m-wide road, eastern area was near a cropland, and western area was near a large cropland with gentle undulations. The position of the grassland made a relatively closed landscape. Thus, we could assume that all the grasshopper individuals moved within this landscape and swarming across the landscape was not considered.

The average elevation was 1339 m, with considerable variation. The landscape was composed of different patches including a small residential area in the southeast, two roads between the western and eastern areas and northern and southern areas, and grasslands with different habitats (especially terrain and vegetation). The plants species were dominated by *S. krylovii*, *Artemisia frigida* Willd., and *Convolvulus ammannii* Desr. during the early growing season. *L. chinensis*, *C. squarrosa*, *A. cristatum*, and *Salsola collina* Pall.

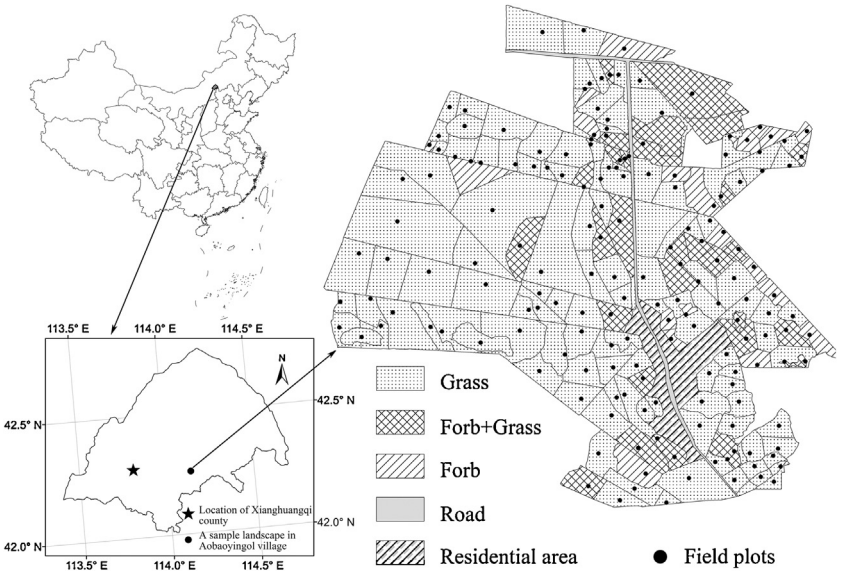

Fig. 2. Location of the study area and a sample landscape in Aobaoyingol village of Xianghuangqi County, Inner Mongolia, China. There are 177 field patches.

were also present. After late July, *S. grandis* could gradually become a subdominant or dominant species at some sites.

We identified 177 grassland patches, each with similar habitats. The landscape represented variations in the spatial aggregation of habitat patches with different suitability levels. We surveyed the size, location, and spatial distribution of each patch using global positioning systems (GPS), and plotted a patch map (Fig. 2). Three field surveys were conducted within each patch in early-July before grasshoppers started to disperse, late-July after grasshoppers could have dispersed, and mid-August at the end of growing season, respectively. During each survey, grasshopper density and some associated habitat conditions were measured within each patch, and these measurements were assumed consistent over the entire patch.

Two or three observers walked side-by-side from the start to the end location within each patch, in the same direction, to visually count the number of *O. d. asiaticus* per m^2. These data were used to estimate the mean density for the patch.

At the center of each patch, we measured the elevation using GPS, and determined the slope and aspect using a compass. Plant species richness, phenology, and vitality were recorded for each patch. Total vegetation (TVC) and grass (GC) coverage were visually estimated within three 1 m × 1 m quadrats, where the soil and vegetation conditions were representative of the patch, and their averages denoted the values for a patch. Soil type was initially determined visually and by feeling the soil by hand. SVWC in the top 5 cm of the soil was measured for the three quadrats of each patch using a soil moisture meter (TDR 300), and the average of the quadrats denoted SVWC for a patch. The 307 soil samples were taken from the top 5 cm of the soil within the landscape. The soil sand content, organic matter content, and pH of these samples were measured using the general methods in the laboratory, and their average denoted the values for a patch. We also surveyed the structure and distribution of gravel and sand within each patch and the intensity and frequency of livestock grazing at the landscape.

3.2. Model parameterization and calibration

3.2.1. Cellular space, neighborhood, and time

The relatively closed landscape was defined as a cellular space. According to Moran's *I* correlogram of *O. d. asiaticus* density, the site size of 30 m × 30 m was smaller than the characteristic scale of local dispersal (180 m × 180 m), so it was reasonable to use the site as a homogeneous spatial cell. The landscape was composed of 13,958 cells of 30 m × 30 m.

The eight-neighbor rule was used. The neighborhood range was 0–64 m, smaller than the actual distance influenced by a focal cell (180 m).

The study was carried out for 42 days from 3 July to 13 August, 2012, spanning the stages from the 2nd instar nymphs to the adult *O. d. asiaticus*. Daily densities of *O. d. asiaticus* were simulated.

3.2.2. Cell states

3.2.2.1. Grass aboveground biomass. The value of G_{ij}^{t} from July 3 to August 13, which was dependent on natural population growth, grasshopper food consumption, and livestock grazing, was obtained from Eq. (5). According to our measured data inside a fenced plot in the study area that contained the same dominant plant species as in the sample landscape in 2012, the periods during which *G* increased, remained constant, and then declined from July 3 ($t = 0$, t_0) to July 15 ($t = 12$, t_1), July 16 to July 25 ($t = 22$, t_2), and July 26 to August 13 ($t = 42$, t_3), respectively.

To obtain aboveground biomass and associated parameters that were not measured at the patches, we selected two sample plots. Both the plots were composed of 5 × 5 contiguously distributed sites, of which each was 30 m × 30 m. The plots were dominated by the same plant species as those in the sample landscape, and had similar seasonal variations in dominant or subdominant plant species to the landscape. Grasshopper density and habitat conditions were measured within each site on July 3 ($t = 0$), July 24 ($t = 21$), and August 9 ($t = 37$), 2012, respectively, using the same methods as those within the patches of the landscape. In one of the three quadrats used for measuring TVC and GC, all the standing live aboveground plants were cut from the base of the plants and placed in different paper bags labeled with the plant names. After the samples were air dried, they were oven dried at 80 °C for 10 h, after which they were weighed using an electronic scale to the closest 0.01 g.

The regression relationships between GC (or TVC) and grass biomass (*G*) and total aboveground biomass (TAB) during the three surveys were respectively built based on the 50 measured data at the two sample plots. TVC at a cell was inversed from the NDVI at the cell and the maximum and minimum NDVI over the entire landscape. *G* and TAB at each cell were estimated using the inversed TVC and the derived biomass-coverage relationships above. In the

Table 1
Amount eaten, duration of growth, and survival rate of *Oedaleus decorus asiaticus* during different instars in 2012. Data were obtained by Huihui Wu, Institute of Plant Protection, Chinese Academy of Agricultural Sciences, who measured inside a fenced plot that contained the same dominant plant and grasshopper species as in the sample landscape in 2012. *O. d. asiaticus* became 2nd instar nymphs on July 1, 2012, and the 2nd instar lasted about 9 days.

Developmental stage	Amount eaten [$k(t)$] (g ind^{-1} d^{-1})	Duration of growth	Time in the model (t)	Survival rate (%)
2nd instar nymph	0.0135	July 3–9	t = 0–6	80.87%
3rd instar nymph	0.0355	July 10–17	t = 7–14	80.87%
4th instar nymph	0.0694	July 18–27	t = 15–24	85.73%
5th instar nymph	0.182	July 28–August 2	t = 25–30	100.00%
Adult	0.148	August 3–13	t = 31–37	–

Table 2
Comparison between the modeled and measured density of *Oedaleus decorus asiaticus*.

Initial grasshopper density (GD)	Number of cells	Modeled GD (mean ± standard deviation)		Difference between the mean measured and modeled GD (ind m^{-2})		Percentage of cells with the difference <2.5 ind m^{-2} (%)	
		Late-July	Mid-August	Late-July	Mid-August	Late-July	Mid-August
GD > 10	242	4.84 ± 2.41	4.51 ± 2.61	−0.27	0.71	80.17	74.79
5 < GD ≤ 10	4064	3.21 ± 1.87	2.92 ± 1.91	−0.40	0.23	64.03	70.25
1 ≤ GD ≤ 5	9183	1.61 ± 1.10	1.49 ± 1.23	0.89	1.38	72.68	65.97
GD = 0	469	0.63 ± 1.57	1.26 ± 2.25	0.97	2.12	95.74	34.75
Total	13,958	2.09 ± 1.13	1.95 ± 1.31	0.48	1.06	71.06	66.32

logistic equation (3), K was set at 92.95 g m^{-2}, from the estimated maximum G during the entire growing season that was studied. The value of r was equal to 0.28, calibrated according to the natural growth of grasses. The values of f_{ij}^1 and f_{ij}^2 were calculated from the estimated G and TAB within cell B_{ij}.

The values of β_{ij}^1 and β_{ij}^2 ranged from 0.45 to 2.35 g m^{-2} d^{-1} and were calculated from the statistical materials from Xianghuangqi County grassland station and personal communication with the staff at the station. The values of γ_{ij} were between 0.4 and 0.8 g m^{-2} d^{-1} and were based on the natural growth and withering of plants and our measured aboveground biomass at the sample plots. The values of β_{ij}^1, β_{ij}^2, and γ_{ij} were first generated from a random function and then calibrated manually. The calibration was to ensure that the difference between the modeled and estimated $G_{ij}^{t=21}$ from GC or TVC, and between the modeled and estimated $G_{ij}^{t=37}$ from GC or TVC did not exceed 2.5 g m^{-2}.

3.2.2.2. Density of Oedaleus decorus asiaticus. The densities of *O. d. asiaticus* measured within the 177 patches in early-July were considered the initial densities (N_{ini}). It was assumed that all the cells within a patch had the same N_{ini}. The cells with N_{ini} of <2, 2–5, 5–10, and ≥10 ind m^{-2} accounted for 16.35, 52.63, 29.15, and 1.87%, respectively.

The variation in daily density from July 3 to August 13 depended on demographic processes, grasshopper–plant interactions, and dispersal processes among the adjacent cells. Biological properties associated with demographic processes such as amount eaten, duration of growth, feeding habits, and survival rate of *O. d. asiaticus* during different instars were assumed the same for all the cells (Table 1).

3.2.3. Dispersal rules

The principles have been given above, except that some parameters should be specified to realize the dispersal rules.

To determine source and sink cells, the cells with high, medium, and low habitat suitability were assigned the threshold densities of *O. d. asiaticus* (N_{ts}) of 10, 5, and 2 ind m^{-2}, respectively, following our measured data, and the threshold grass aboveground biomass (G_{ts}) was 5.0 g m^{-2}.

We integrated the model system built by Shen et al. (2015) and Zhang et al. (2015) to evaluate the grasshopper habitat suitability. The evaluation was made for each cell based on the measured habitat conditions including elevation, slope, aspect, SVWC, vegetation type, and TVC, the interpolated soil sand content, soil organic matter content, and soil pH using the kriging method, and digital elevation map (DEM) (spatial resolution of 30 m × 30 m) and soil type map (cartographic scale of 1:1,000,000). The data measured in early-July were used to evaluate habitat suitability for each cell from the early to peak growing season (July 3–23), and the data measured in late-July were used for each cell from the peak to late growing season (July 24–August 13). Using the field patch data in early-July, averages of the measured grasshopper densities within the cells with high, medium, and low habitat suitability over the entire landscape, AGD_3, AGD_2, and AGD_1, were 10.6, 5.9, and 2.4 ind m^{-2}, respectively. Thus, P_3, P_2, P_1, p_3, p_2, and p_1 from the early to peak growing season (July 3–23) were estimated as:

$$\begin{cases} P_3 = 10.6/(10.6S_3 + 5.9S_2 + 2.4S_1) \\ P_2 = 5.9/(10.6S_3 + 5.9S_2 + 2.4S_1) \\ P_1 = 2.4/(10.6S_3 + 5.9S_2 + 2.4S_1) \\ p_3 = 10.6/(10.6s_3 + 5.9s_2 + 2.4s_1) \\ p_2 = 5.9/(10.6s_3 + 5.9s_2 + 2.4s_1) \\ p_1 = 2.4/(10.6s_3 + 5.9s_2 + 2.4s_1) \end{cases} \quad (14)$$

Similarly, the migrating probabilities from the peak to the late growing season were estimated on the basis of the grasshopper densities measured in late-July over the entire landscape with the corresponding habitat suitability.

4. Simulation results

4.1. Evaluation of estimation accuracy

The mean modeled density of *O. d. asiaticus* was 0.48 ind m^{-2} lower than the mean measured density in late July. For the cells with nymphs at time t_0, the differences between the mean measured and modeled densities were <0.90 ind m^{-2}, and the differences were lower than 2.5 ind m^{-2} for more than 64% of these cells (Table 2). The modeled densities were within the measured ranges for 93.5% of cells, and could explain 60.6% of the variance (Fig. 3).

The mean modeled density of *O. d. asiaticus* was 1.06 ind m^{-2} lower than the mean measured density in mid-August. For the

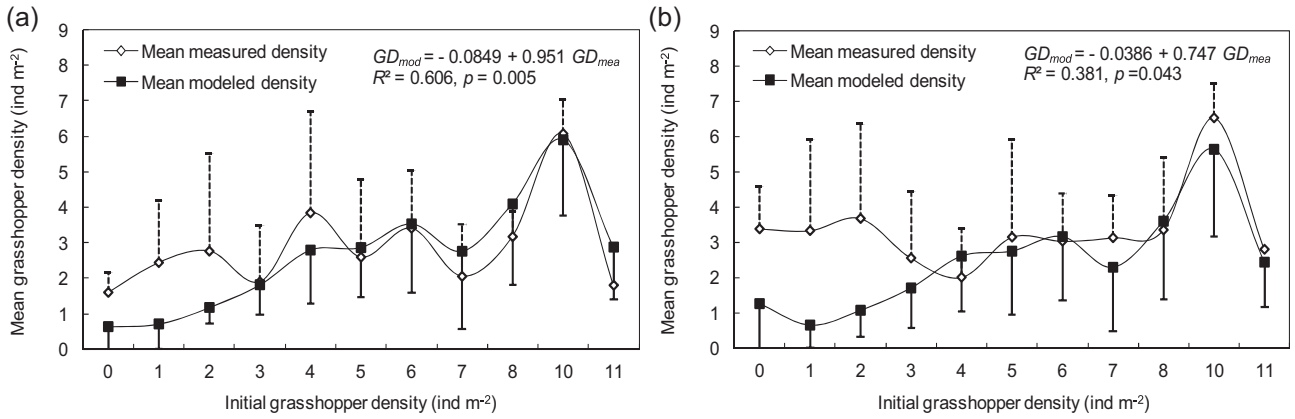

Fig. 3. Comparison between the mean modeled (GD_{mod}) and measured density (GD_{mea}) of *Oedaleus decorus asiaticus* in late July (a) and mid-August (b). Positive and negative standard deviation error bars are provided for GD_{mea} and GD_{mod}, respectively. The numbers of the cells for the initial densities of 0, 1, 2, 3, 4, 5, 6, 7, 8, 10, and 11 are 469, 1819, 2015, 3946, 1403, 1856, 1012, 566, 630, 157, and 85, respectively.

cells with nymphs at time t_0, the differences between the mean measured and modeled densities were <1.40 ind m^{-2}, and the differences were lower than 2.5 ind m^{-2} for more than 65% of these cells (Table 2). The modeled densities were within the measured ranges for 66.6% of cells, and could explain 38.1% of the variance (Fig. 3).

The estimation accuracy was higher for the 4th and 5th instars than for the adulthood (Fig. 3 and Table 2), because more uncertain factors (such as strong wind or suddenly declining temperature) might influence grasshopper survival after early-August, but they were not considered in the model.

The estimation accuracy was higher for cells with higher initial densities (Fig. 3 and Table 2). For cells with the initial densities lower than 3 ind m^{-2}, the modeled densities were around 1.5–2.5 ind m^{-2} lower than the measured ones (Fig. 3). More than 83% of these cells had high or medium habitat suitability, resulting in high probabilities of attracting more individuals during and after the 4th instar. However, the densities within most of these cells and their neighboring cells were always lower than the threshold densities corresponding to habitat suitability levels, so most of these cells became sink cells. The lack of source cells resulted in low immigration for these sink cells. In addition, a small amount of grasshopper individuals more easily causes a measurement error. In the field, individuals might not exist within some sites and aggregate within other sites. This uneven distribution made accurate measurement impossible. Increasing or decreasing individuals could produce considerable differences in statistics when there are few individuals per m^2.

4.2. Modeled spatiotemporal variation in grasshopper density

The results showed that the modeled *O. d. asiaticus* density declined throughout the growing season (Figs. 4 and 5). However, the densities exhibited different temporal variations for the cells with different initial densities.

For the cells with nymphs at time t_0, *O. d. asiaticus* density remained constant during the whole 2nd instar (July 3–9) and 3rd instar (July 10–17) (Fig. 4a and b), because nymphs moved only within the source cells and could not disperse to other cells, and the CA model assumed that they all survived during a given instar. For the 469 cells without nymphs at the time t_0, the empty situation lasted during each of these two instars (Fig. 4c), even if the cells were suitable for nymphs.

During the 4th instar (July 18–27), *O. d. asiaticus* could move to more suitable cells. This movement caused *O. d. asiaticus* densities within some cells to exhibit fluctuating variations around

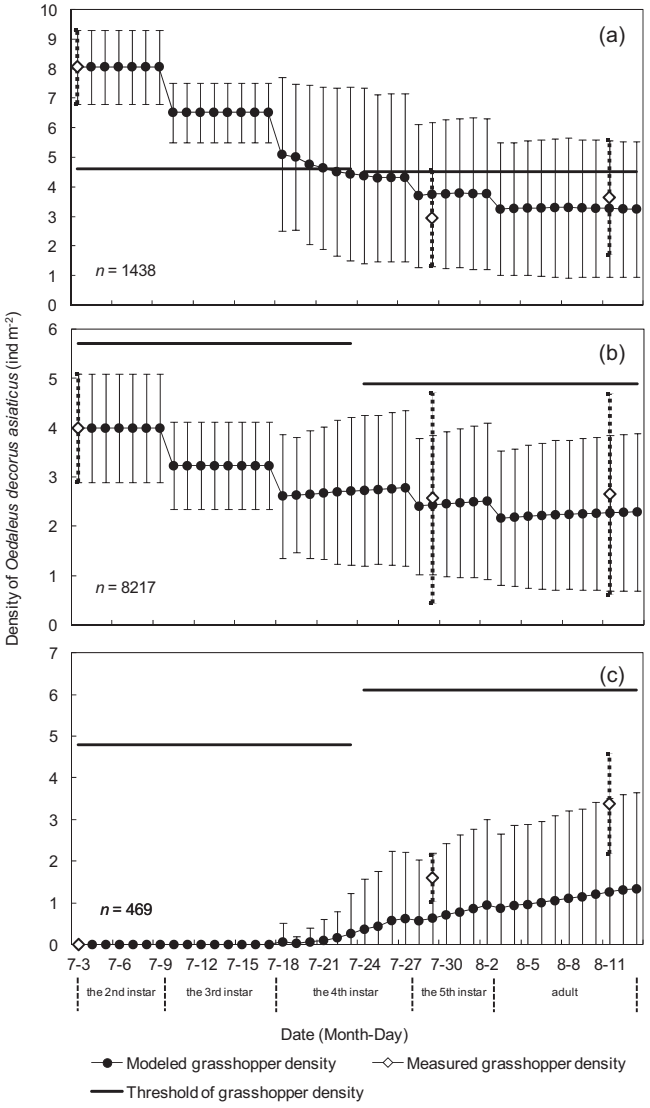

Fig. 4. Temporal variations in the modeled average density of *Oedaleus decorus asiaticus* for the cells with the initial density of 7–12 ind m^{-2} (a), 3–6 ind m^{-2} (b), and 0 ind m^{-2} (c), as the case study in 2012. Standard deviation error bars are provided for the modeled and measured densities using the solid line and dot-dashed line, respectively.

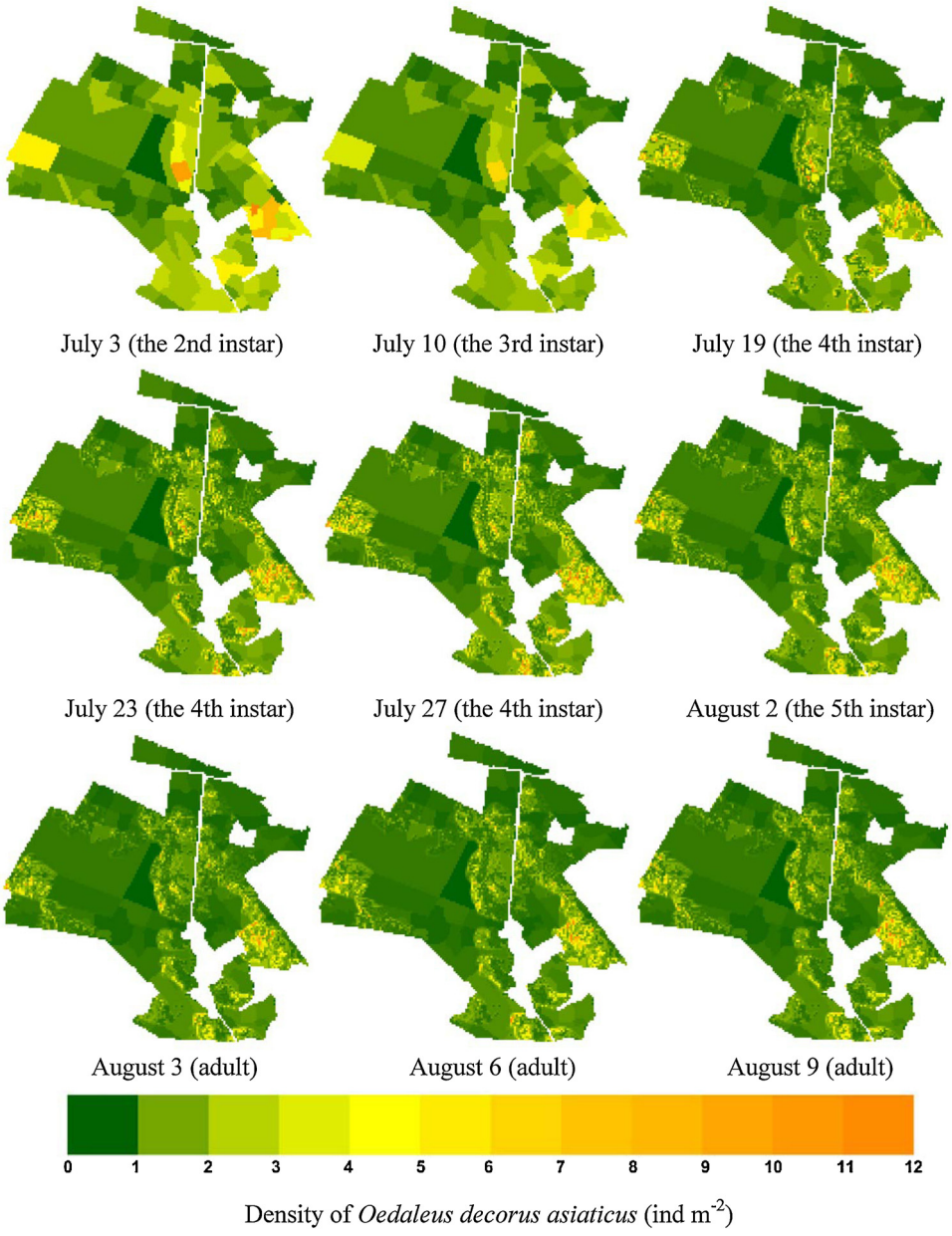

Fig. 5. Spatiotemporal variations in modeled density of *Oedaleus decorus asiaticus* for all the cells within the sample landscape in 2012.

the corresponding threshold values. For the cells with initial densities >6.0 ind m^{-2}, the densities at the end of the 3rd instar mostly exceeded their threshold values, some individuals could emigrate from these cells. Hence, *O. d. asiaticus* density rapidly declined during the 4th instar (Fig. 4a).

In contrast, for cells with the initial densities <6.0 ind m^{-2}, the densities at the end of the 3rd instar were mostly below their threshold values, some individuals from adjacent cells could immigrate to these cells. Hence, *O. d. asiaticus* density increased during the 4th instar, even during the 5th instar and adulthood (Fig. 4b). In particular, for the empty cells at time t_0, the densities of late-instar nymphs and adults increased linearly after the 3rd instar (Fig. 4c).

During and after the 5th instar (from July 28 to August 13), around 11% cells experienced a decrease in habitat suitability, while others varied negligibly. The correspondingly slightly decreasing threshold densities were still greater than most of the modeled densities, which greatly reduced their fluctuations making them very stable (Figs. 4 and 5). In addition, weather changes (especially declining temperature) affected the survival of *O. d. asiaticus*. Several adults died after they spawned.

The overall spatiotemporal variations in the modeled *O. d. asiaticus* densities over the entire landscape, and the differences between different instars, agreed with the actual observed trend in the field (Figs. 4 and 5). The modeled *O. d. asiaticus* densities were mostly within the measured ranges during and after the 4th instar, when the densities were most likely to change (Fig. 4).

4.3. Modeled grass aboveground biomass and relationship with grasshopper density

When livestock grazing and grasshopper food consumption were not considered, the grass aboveground biomass within all the cells increased following the general logistic curve during the early and peak growing season, biomass remained approximately invariant for about 10–20 days after it reached the peak, and biomass gradually decreased after that point. However, the actual biomass trends differed greatly from the ideal ones, because the sampled

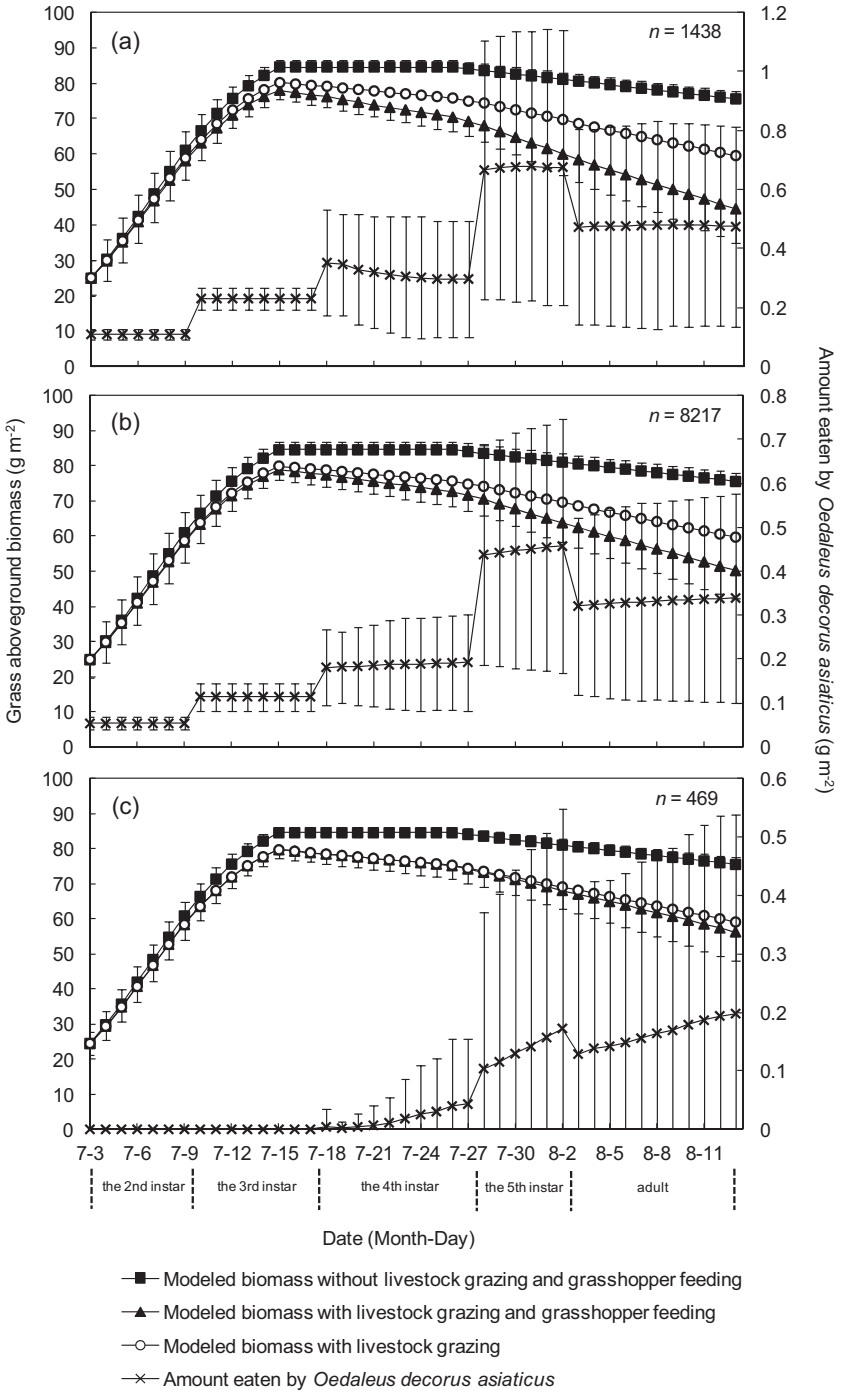

Fig. 6. Temporal variations in the mean estimated amount of material eaten by *Oedaleus decorus asiaticus* and mean modeled grass aboveground biomass under different conditions of disturbance for the cells with the initial density of 7–12 ind m^{-2} (a), 3–6 ind m^{-2} (b), and 0 ind m^{-2} (c), as the case study in 2012. Standard deviation error bars are provided.

landscape was moderately or severely grazed and was affected by a certain amount of grasshoppers. Compared with the ideal trends, the biomass peaks also occurred in mid-July, and the peaks were smaller than the carrying capacity K (92.95 g m^{-2}); biomass decreased gradually and continuously after it reached the peak, without having a stable period (Fig. 6).

The amount of grasses eaten by *O. d. asiaticus* increased with the instar and peaked during the 5th instar for most of the cells (Fig. 6). During the same instar, the amount consumed was positively correlated with *O. d. asiaticus* density (Figs. 4 and 6).

The measured and modeled data showed that there was no obvious correlation between the *O. d. asiaticus* density and the grass aboveground biomass during the 2nd and 3rd instars because of low amount eaten within all the cells, regardless of density. After becoming adults, *O. d. asiaticus* did not feed on a number of grasses because the densities were lower than 3.0 ind m^{-2} within about 80% of the cells. Even during the 4th and 5th instars, there was no obvious correlation between the grasshopper density and grass biomass, because grass biomass was not one of the main factors limiting the survival of *O. d. asiaticus* for most of the cells.

Kang and Chen (1995) found that the interactions between the grasshopper and plant community significantly affected the composition and structure of plant and grasshopper communities. However, Kang determined that the varying trends were not always synchronous, because suitable habitat sites and refuges that plants provide to grasshoppers could be more important to grasshopper populations than the food that the plants provide, especially when a large amount of preferred plants are available. Only if there are very few plants does food become a critical factor. Although our study was conducted at the population rather than community level, we reached similar conclusions.

5. Discussion

The CA model offers a new approach that reveals the spatiotemporal dynamics of grasshopper populations in a typical semiarid steppe. The model provides a basic perspective on the interactions between spatial patterns and ecological processes at multiple spatial extents (namely, cell and cellular space) in a heterogeneous area. Unlike other insect diffusion models, the present CA model accounts for heterogeneity in all the design principles. Within a cellular space, the spatial pattern of grasshopper density mainly depended on the spatial heterogeneity of habitat factors including terrain, soil, and vegetation aspects, which was the basic condition for spatial movement. It also depended on the interactions between plants and grasshopper individuals, which were spatially heterogeneous because grass biomass varied at different cells. Besides habitat suitability and grasshopper-plant relationships, the distance from a source to sink cell (position relationship) was another important factor. All these aspects finally determined the spatial heterogeneity of grasshopper density over the entire cellular space.

The present CA model differs from most previously developed CA models in two ways. First, since most CA models have been deterministic, in our model the rules describing both the total number of individuals moving to neighboring cells and their allocation to cells with different habitat suitability levels are probabilistic. It would be difficult to use a deterministic equation set to describe unique cells, their heterogeneous attributes and behaviors, and their interactions. The incorporation of the stochastic approach has considerable advantages for modeling these heterogeneities and uncertain complex dispersal processes (Bian, 2013). Secondly, the states of a cell involve grasshopper density and grass biomass, and individuals spread through the space by two mechanisms: grasshopper–plant interactions within a cell and interactions between adjacent cells by dispersal processes. The approach improves the simulation of the synergic relationship between grasshoppers and grasses.

In the case study, the data from the sample landscape are independent from those at the 150 m × 150 m plots, from which partial parameters were obtained. The validation of the model indicated that this type of CA model identified and captured the essential spatiotemporal patterns and underlying processes, causing no qualitative abnormity in population-level behaviors. Therefore, the model is useful for predicting the spatiotemporal dynamics of grasshopper (or other motile pest) populations in a heterogeneous space.

However, it should be noted that the present CA model is most effective if applied to an *O. d. asiaticus* population whose initial density is 3–12 ind m^{-2} after hatching. Under these circumstances, grasshoppers and plants coexist within the same space, and individuals disperse among adjacent cells or patches rather than swarming across landscapes. Thus, spatial isolation and environmental heterogeneity within patches or landscapes could strongly influence dispersal processes among adjacent cells or patches and grasshopper–plant interactions. On the contrary, for grasshopper outbreaks, strong demographical stochasticity, transient dynamics, and long-distance swarms may occur, and grasses could become extinct at any time. Thus, spatial heterogeneity within a patch or landscape affects swarming processes across landscapes only to a small degree, because of their mismatch in scales. Alternative model rules will have to be drawn for this case. However, the present CA model could potentially generate the dynamics leading to a transition to swarming. It will depend on determining the threshold of grasshopper–plant interactions in a larger space. A CA-based metapopulation model rather than a CA model itself could be well suited to modeling long-distance migration (Vinatier et al., 2011), or multi-scale models could be developed by coupling a small-scale CA model with a large-scale reaction-diffusion model (Ciss et al., 2013).

At almost every step of the construction of this CA model, at least a few alternative approaches are plausible. How does a choice from among these alternatives change spatiotemporal patterns of grasshopper populations? Murdoch et al. (1992) suggested constructing a suite of models with increasing complexity and then choosing the appropriate alternative for a given application. This issue is beyond the theme of this paper, but should be discussed.

Some alternatives are given for the design principles and assumptions. The assumptions underlying an ecological model aim to simplify rules while extracting the main components and features and capturing key processes under the constraints of current observation and data conditions. However, some assumptions may inherently reduce model realism and adaptability.

The present CA model assumes that the cellular space is a relatively closed system, composed of discrete square cells. However, it is an open system, and the *O. d. asiaticus* individuals near the space boundary could have stronger interactions with their surroundings than with the interiors. The individuals leaving the space may be lost and thus reduce the population size, a phenomenon called the boundary effect (Berec, 2002). This effect depends on spatial extent and is especially apparent in a finite space. In our case study, the space was a large enough landscape so that this effect was reliably weakened. We expect to eventually extend it to a region (such as Xianghuangqi County) composed of respective landscapes, and replace the regular cells with subpopulation patches that have irregular shapes and may change with time.

The present CA model assumes that *O. d. asiaticus* individuals and plants homogeneously distribute within a cell. We observed apparent variations in grasshopper density even within a 30 m × 30 m cell; and some plant species occurred in patchy distributions rather than random or uniform distributions. Quantifying spatial heterogeneity within a cell, decreasing cell size, or using individual-based CA models may address this issue, if sufficient detailed information is available.

The present CA model assumes that interactions only occur within the neighborhood. However, individuals within a cell in a social network may interact with others that are not necessarily spatially adjacent. The structure of the social network determines how individuals propagate through space. Commonly considered structural factors include the number of individuals with interactions (emigration and immigration), the frequency and range of interactions, the connections among cells, and the cross-connections within a group of cells (Ghani et al., 1997).

The present CA model assumes that during each instar *O. d. asiaticus* individuals in the cellular space are homogeneously mixed. However, we observed that individuals of different instars sometimes coexist. Therefore, it may be necessary to explicitly demonstrate the age-structure to differentiate demographic processes.

The present CA model extracted three critical plant growth periods: early growing season (before dispersal), blooming (after dispersal), and late growing season. However, given that these intervals may exceed 10 days, they may be too long to capture

certain processes that affect plant growth and grasshopper development. Hence, shorter-interval data are needed for a complete description of the details of the growing process.

In addition, the study area sometimes experiences extreme or unusual weather such as heavy drought, rainstorms, strong winds, and low temperatures. Hence, it may be necessary to explicitly demonstrate how weather affects grasshopper survival, growth, and dispersal and plant growth and withering.

There are also other alternatives for technical methods, such as how to evaluate habitat suitability, how to express spatial isolation, and how to define the neighborhood of a cell.

In the model system proposed by Shen et al. (2015) and Zhang et al. (2015), the effects of habitat factors on grasshopper density were globally estimated over the entire sample area, and were used for each cell in the present CA model. However, these effects may vary for different cells, exhibiting strong spatial heterogeneity. We will use an improved geographically weighted regression method to obtain the local effects.

The present CA model expresses isolation using the simple Euclidean distance from the center of a cell to the center of another cell, which is a physical rather than a functional distance related to the costs paid by *O. d. asiaticus*. Patchy distribution of many plants that are not eaten by *O. d. asiaticus* (such as *C. ammannii* and *A. frigid*) could become an obstacle that limits individual dispersal between cells. Therefore, it is necessary to quantify the effect of spatial configuration of different plant species on dispersal processes in future studies.

In addition, the neighborhood definition may be expanded beyond the nearest cells if it is below dispersal range, as shown in the Supplement materials.

In summary, the CA model we constructed serves as an important foundation for future development, and alternative approaches may result in more reliable model analyses. Some alternatives may result in a more realistic model that is more complex to formulate, simulate, and analyze. The choice of appropriate alternatives for a given applied issue is a trade-off between realism and computational simplicity (Berec, 2002); therefore, the most appropriate model will have to take this into consideration.

Acknowledgments

This research was financially supported by the National Natural Science Foundation of China (grant no. 31270512). We would like to thank the staff members from the Xianghuangqi County Grassland Station, Xilingol League, and Zehua Zhang and Huihui Wu from the Institute of Plant Protection, Chinese Academy of Agricultural Sciences, for their help conducting the field survey and data collection. We gratefully acknowledge six undergraduate students, Jun-Qi Hu, Wu-Xia Gao, Jian-Kai Xu, Fei Feng, Yu-Long Zheng, and Yu-Sheng Liang, from Northwest A & F University, for their field work. We also gratefully acknowledge the editor and anonymous reviewers for their valuable comments and constructive suggestions. Finally, we would like to thank Editage (http://www.editage.cn/index.html) for English language editing.

Appendix A. Supplementary data

Supplementary data associated with this article can be found, in the online version, at http://dx.doi.org/10.1016/j.ecolmodel.2016.03.002.

References

Blackwell, P.G., 2007. Heterogeneity, patchiness and correlation of resources. Ecol. Model. 207, 349–355.

Balzter, H., Braun, P.W., Kohler, W., 1998. Cellular automata models for vegetation dynamics. Ecol. Model. 107, 113–125.

Berec, L., 2002. Techniques of spatially explicit individual-based models: construction, simulation, and mean-field analysis. Ecol. Model. 150, 55–81.

Bian, L., 2013. Spatial approaches to modeling dispersion of communicable diseases – a review. Trans. GIS 17, 1–17.

Bone, C., Dragicevic, S., Roberts, A., 2006. A fuzzy-constrained cellular automata model of forest insect infestations. Ecol. Model. 192, 107–125.

Cannas, S.A., Paez, S.A., Marco, D.E., 1999. Modeling plant spread in forest ecology using cellular automata. Comput. Phys. Commun. 121–122, 131–135.

Chen, Q.W., Han, R., Ye, F., Li, W.F., 2011. Spatio-temporal ecological models. Ecol. Inform. 6, 37–43.

Chen, S.H., Wulanbater, Cao, Y.F., 2006. Effects of climatic change on grassland locust in Inner Mongolia. Pratacult. Sci. 23 (8), 78–82 (in Chinese).

Chen, Y.L., 2007. Ecological Management of Main Grasshoppers and Grasshopper Plagues in China. Science Press, Beijing (in Chinese).

Ciss, M., Parisey, N., Dedryver, C.A., Pierre, J.S., 2013. Understanding flying insect dispersion: multiscale analyses of fragmented landscapes. Ecol. Inform. 14, 59–63.

Davidson, D.A., Theocharopoulos, S.P., Bloksma, R.J., 1994. A land evaluation project in Greece using GIS and based on Boolean and fuzzy set methodologies. Int. J. Geogr. Inform. Syst. 8 (4), 369–384.

Dungan, J.L., Perry, J.N., Dale, M.R.T., Legendre, P., Citron, P.S., Fortin, M.J., Jakomulska, A., Miriti, M., Rosenberg, M.S., 2002. A balanced view of scale in spatial statistical analysis. Ecography 25, 626–640.

Fan, W.M., Li, H.C., Qiu, X.H., 1997. The concept and calculation methods of grasshopper damage in typical steppes. In: Inner Mongolia Grassland Ecosystem Research Station of Chinese Academy of Sciences (Ed.), Research on Grassland Ecosystem, No. 4. Science Press, Beijing, pp. 283–287 (in Chinese).

Ghani, A.C., Swinton, J., Garnett, G.P., 1997. The role of sexual partnership networks in the epidemiology of gonorrhea. Sex. Transm. Dis. 24, 45–56.

Grimm, V., Revilla, E., Berger, U., Jeltsch, F., Mooij, W.M., Railsback, S.F., Thulke, H.H., Weiner, J., Wiegand, T., DeAngelis, D.L., 2005. Pattern-oriented modeling of agent-based complex systems: lessons from ecology. Science 310, 987–991.

Hogeweg, P., 1988. Cellular automata as a paradigm for ecological modeling. Appl. Math. Comput. 27, 81–100.

Kang, L., Chen, Y.L., 1992. Temporal and spatial heterogeneity of grassland grasshoppers. In: Inner Mongolia Grassland Ecosystem Research Station of Chinese Academy of Sciences (Ed.), Research on Grassland Ecosystem, No. 4. Science Press, Beijing, pp. 109–123 (in Chinese).

Kang, L., Chen, Y.L., 1995. Dynamics of grasshopper communities under different grazing intensities in Inner Mongolian steppes. Insect Sci. 2 (3), 265–281.

Li, X., Ye, J.A., Liu, X.P., Yang, Q.S., 2007. Geographical Simulation Systems: Cellular Automata and Multi-Agent. Science Press, Beijing (in Chinese).

Liu, L., Guo, A.H., 2004. Analysis of meteorological and ecological conditions of grasshopper infestations in Inner Mongolia in 2004. Meteorol. Mon. 30 (11), 55–57 (in Chinese).

Lu, H., Yu, M., Zhang, L.S., Zhang, Z.H., Long, R.J., 2005. Effects of foraging by different instar and density of *Oedaleus asiaticus* B. Bienko on forage yield. Plant Prot. 31 (4), 56–59 (in Chinese).

Ma, S.J., 1964. The structure and dynamics of space, number and time of insect population. Acta Entomol. Sin. 13 (1), 38–55 (in Chinese).

Matsumoto, M., Nishimura, T., 1998. Mersenne Twister: a 623-dimensionally equidistributed uniform pseudo-random number generator. ACM Trans. Model. Comput. Simul. 8 (1), 3–30.

Murdoch, W.W., McCauley, E., Nisbet, R.M., Gurney, W.S.C., de Roos, A.M., 1992. Individual-based models: combining testability and generality. In: De Angelis, D.L., Gross, L.J. (Eds.), Individual-Based Models and Approaches in Ecology-Populations, Communities and Ecosystems. Chapman & Hall, New York, pp. 18–35.

Ni, S.X., 2002. Monitoring and Predicting Grasshopper Infestations in the Regions Around Qinghai Lake by Remote Sensing. Shanghai Science and Technology Press, Shanghai (in Chinese).

Perry, G.L.W., Enright, N.J., 2007. Contrasting outcomes of spatially implicit and spatially explicit models of vegetation dynamics in a forest-shrubland mosaic. Ecol. Model. 207, 327–338.

Pukkala, T., Möykkynen, T., Robinet, C., 2014. Comparison of the potential spread of pinewood nematode (*Bursaphelenchus xylophilus*) in Finland and Iberia simulated with a cellular automaton model. Forest Pathol. 44, 341–352.

Shen, J., Zhang, N., Gexigeduren, He, B., Liu, C.Y., Li, Y., Zhang, H.Y., Chen, X.Y., Lin, H., 2015. Construction of a GeogDetector-based model system to indicate the potential occurrence of grasshoppers in Inner Mongolia steppe habitats. Bull. Entomol. Res. 105, 335–346, http://dx.doi.org/10.1017/S0007485315000152.

Simpson, S.J., McCaffery, A.R., Hagele, B.F., 1999. A behavioural analysis of phase change in the desert locust. Biol. Rev. Camb. Philos. Soc. 74, 461–480.

Torrusio, S., Cigliano, M.M., de Wysiecki, M.L., 2002. Grasshopper (Orthoptera: Acridoidea) and plant community relationships in the Argentine pampas. J. Biogeogr. 29, 221–229.

Vinatier, F., Tixier, P., Duyck, P.F., Lescourret, F., 2011. Factors and mechanisms explaining spatial heterogeneity: a review of methods for insect populations. Methods Ecol. Evol. 2, 11–22.

Wang, J.F., Hu, Y., 2012. Environmental health risk detection with GeogDetector. Environ. Model. Softw. 33, 114–115.

Wang, J.F., Liao, Y.L., Liu, X., 2010. Analysis Tutorial of Spatial Data. Science Press, Beijing, pp. 50–55 (in Chinese).

Wang, J., Kropff, M.J., Lammert, B., Christensen, S., Hansen, P.K., 2003. Using CA model to obtain insight into mechanism of plant population spread in a controllable system: annual weeds as an example. Ecol. Model. 166 (3), 277–286.
Yan, Z.C., Chen, Y.L., 1998. The relationship between morphological character and dispersal ability of grasshoppers in typical steppe (Orthoptera: Acridoidea). Acta Ecol. Sin. 18 (2), 171–175 (in Chinese).
Zhang, N., Zhang, H.Y., He, B., Gexigeduren, Xin, Z.Y., Lin, H., 2015. Spatiotemporal heterogeneity of the potential occurrence of *Oedaleus decorus asiaticus* in Inner Mongolia steppe habitats. J. Arid Environ. 116, 33–43, http://dx.doi.org/10.1016/j.jaridenv.2015.01.019.
Zhou, G.F., Liebhold, A.M., 1995. Forecasting the spatial dynamics of gypsy-moth outbreaks using cellular transition models. Landsc. Ecol. 10 (3), 177–189.
Zhou, X.R., Chen, Y., Guo, Y.H., Pang, B.P., 2012. Population dynamics of *Oedaleus asiaticus* on desert grasslands in Inner Mongolia. Chin. J. Appl. Entomol. 49 (6), 1598–1603 (in Chinese).